

THE "PIERCE"-GEOMETRY
AN ACCELERATING COLUMN DESIGN*

C. Robert Emigh
Los Alamos Scientific Laboratory
Los Alamos, New Mexico

Introduction

The popular trend in today's design of accelerating columns is to make the field gradient near the extraction area as large as possible. The argument has been that if the proton beam energy can be brought up to the accelerator injection level in a very short distance, space charge has little time in which to act to increase the effective emittance by warping the emittance pattern. Support for this argument has come from the success of recently tested short columns in producing proton beams with low normalized emittances, in the region of 0.05 cm-milliradian. It is generally accepted that only the extraction system of Pierce is without aberrations. To emphasize these essential features of the Pierce extraction--coaxial flow, zero angular momentum, and a uniform density distribution--a derivation based on a zero effective emittance pattern throughout the acceleration is presented. Thus the recent successes in generating low emittance beams are probably the result of the "Pierce"-like geometries used by the column designer to implement his high gradient criteria rather than a result of the high gradient itself. The high gradient has the advantage of reducing the beam diameter to a manageable size for a given current.

A simple integral equation for the field required outside the beam to support the Pierce geometry is derived. The equation is exact, based only on the $4/3$ power law potential gradient at the beam boundary and on Laplace's equation outside the beam.

Pierce Extraction

Zero Emittance

For the moment consider an idealized approach and assume that the beam is to be accelerated under conditions of zero emittance. In addition, the zero emittance pattern in r - r' phase space should remain linear for all values of z to insure that the effective emittance also will be zero during acceleration; that is, the emittance pattern is not warped. For example, Fig. 1 shows on the upper graph, a zero emittance linear pattern; and shows on the lower graph, a zero emittance non-linear pattern, the effective emittance being perhaps defined by the area of an ellipse which will just enclose the zero emittance pattern. These two assumptions (zero emittance and linearity) are sufficient to establish that the flow is laminar and the current density distribution in real space remains the same throughout the acceleration. This is illustrated in Fig. 2. The continuous line represents one trajectory within the beam, while the dashed line represents any other trajectory within the beam. It is evident that all trajectories are related by simple scaling

factors. Thus any equation representing a beam trajectory must have its boundary conditions such that the equation is independent of r when ar is substituted for r .

Coaxial Beam Trajectories

A time-independent spatial description^{1,2} of individual particle trajectories within a beam having a given current density distribution and under the constraints of an externally applied electric and magnetic axially symmetric field is given by

$$r'' = \frac{[1 + (r')^2]}{2(e\phi^{**})} \left(\frac{\partial(e\phi^{**})}{\partial r} - r' \frac{\partial(e\phi^{**})}{\partial z} \right) \quad (1)$$

where
$$e\phi^{**} = e\phi - \frac{c^2}{2E_0} \left(\frac{c}{r} + eA \right)^2$$

and
$$C = \frac{r^2 \theta' (e\phi^*)^{1/2}}{[1 + r^2 \theta'^2 + (r')^2]^{1/2}} \frac{(2E_0)^{1/2}}{c} - e r A_\theta \quad (2)$$

Also $e\phi^* = e\phi + \frac{(e\phi)^2}{2E_0}$ is the "effective" electric

potential energy and $e\phi$ is normalized so that it is equivalent to the kinetic energy of the particle. In the above equations r , z , and θ are the usual cylindrical coordinates and A is the magnitude of the magnetic vector potential, including both beam self fields and externally applied fields. The prime indicates a differentiation with respect to z . E_0 is the rest energy of the particle, e the charge on the particle, and c the velocity of light. A detailed inspection of the r dependence of the various terms in equations (1) and (2) will show that the set of conditions needed to meet the scale change criterion developed in the preceding paragraph is that r' , r'' , θ' , and $\frac{\partial(e\phi^{**})}{\partial r}$ must be zero everywhere in the beam. Thus the beam trajectories must be coaxial to insure an absolute zero emittance pattern.

Zero Angular Momentum

Equation (2) can be expressed in more familiar terms by recognizing that the angular momentum is

*Work performed under the auspices of the U. S. Atomic Energy Commission.

Pierce Geometry

$$r_{p\theta} = \frac{m_0 r_{\theta}^2 \dot{\theta}}{(1-v^2/c^2)^{1/2}} = \frac{m_0 c^2}{c} \cdot r_{\theta}^2 \theta' \cdot \frac{v}{c} \cdot \frac{v}{c(1-v^2/c^2)^{1/2}}$$

$$r_{p\theta} = \frac{(2E_0)^{1/2}}{c} \frac{(e\phi^*)^{1/2}}{[1 + r_{\theta}^2 \theta'^2 + r'^2]^{1/2}} r_{\theta}^2 \theta' \quad (3)$$

Making this substitution into equation (2), it can be written in the form

$$C = r_{p\theta} - erA_{\theta} \quad (4)$$

From our criterion that $\frac{\partial}{\partial r}(e\phi^{**}) = 0$ everywhere in the beam, or equivalently that $e\phi^{**}$ must be independent of r , it is noted from equation (1) that the constant C must be zero. If it is not, equation (4) shows that a particle emitted in a magnetic field will attain mechanical angular momentum when leaving the field. Thus it is important that at the plasma surface, where the protons are extracted into the accelerating column, there are no magnetic fields which will contribute to the non-linear emittance pattern.

Uniform Density Distribution-Child's Law

The fact the $e\phi^{**}$ must be independent of r , also implies that $e\phi$ must be independent of r . From Poisson's equation

$$\frac{1}{r} \frac{\partial}{\partial r} \left(r \frac{\partial}{\partial r} (e\phi) \right) + \frac{\partial^2}{\partial z^2} (e\phi) = - \frac{e\rho}{\epsilon} \quad (5)$$

it is quite clear that the charge density (or current density) also must be independent of r . Therefore equation (5) reduces to

$$\frac{\partial^2}{\partial z^2} \phi = - \frac{\rho}{\epsilon} \approx \frac{J}{\epsilon} \left(\frac{m_0}{2e} \right)^{1/2} \frac{1}{\phi^{1/2}} \quad (6)$$

where only the relativistic mass correction is assumed to be negligible. This differential equation can be solved easily for ϕ , the required potential distribution within the beam, and yields the familiar Child-Langmuir space charge law.

$$\phi = \alpha Z^{4/3}, \text{ where } \alpha = \left[\frac{9J}{4\epsilon} \left(\frac{m}{2e} \right)^{1/2} \right]^{2/3} \quad (7)$$

External Fields

The ideal approach to an accelerating column is to accelerate a uniform density beam according to the 4/3 power law, as outlined in the preceding paragraphs. Under these conditions the potential within the beam is independent of radius and as a result there are no forces present internal to the beam to warp the emittance pattern. The field necessary outside the beam to support this 4/3 potential gradient along the beam has not been calculated theoretically except for the semi-infinite rectangular beam and for the infinitely thin line current. The geometrical design criteria for the circular beam "Pierce gun" is usually developed experimentally from electrolytic tank measurements. Therefore, it is of both academic and of practical interest to attempt a theoretical approach to this problem.

Consider a uniform density beam of radius ρ formed by a parallel flow of particles being emitted from a plane plasma surface at zero energy and being accelerated by a series of equipotential surfaces formed in such a manner that the energy gain obeys the required 4/3 power law. In order that the radial forces at the edge of the beam be zero, the radial potential gradient at the edge of the beam also must be zero. Thus our boundary conditions are

$$\begin{aligned} \text{a. } & V(R,Z) = \alpha Z^{4/3} \quad \text{at } R = 1 \\ \text{b. } & \frac{\partial V(R,Z)}{\partial R} = 0 \quad \text{at } R = 1 \end{aligned} \quad (8)$$

where R and Z are dimensionless units r/ρ and z/ρ respectively and where ρ is the radius of the beam. Outside of the boundary, where $R > 1$, the potential everywhere must obey Laplace's equation

$$\frac{1}{R} \frac{\partial}{\partial R} \left\{ R \frac{\partial}{\partial R} V(R,Z) \right\} + \frac{\partial^2}{\partial Z^2} V(R,Z) = 0. \quad (9)$$

The form of the solution of this equation which is appropriate to our boundary conditions can be obtained by a separation of variables; that is, $U(R) W(Z)$ is a solution to Laplace's equation where

$$U(R) = a(k) J_0(kR) + b(k) Y_0(kR) \quad (10)$$

$$\text{and } W(Z) = e^{-kZ}$$

and where k is an arbitrary variable. Here $J_0(kR)$ is a Bessel function of the first kind of order zero, and $Y_0(kR)$ is a Bessel function of the second kind of order zero. We now ask that $U(R) = 1$ for $R = 1$ and $\frac{\partial}{\partial R} U(R) = 0$ for $R = 1$. Therefore

$$a(k) J_0(k) + b(k) Y_0(k) = 1$$

$$\text{and } -a(k) k J_1(k) - b(k) k Y_1(k) = 0.$$

Solving these two equations simultaneously, we find

$$U(R) = \frac{\pi k}{2} \{ J_1(k) Y_0(kR) - Y_1(k) J_0(kR) \}. \quad (11)$$

We are now able to write the entire solution for $Z \geq 0$ in terms of our arbitrary variable

$$V(R,Z) = \int_0^{\infty} c(k) U(R) e^{-kZ} dk$$

$$\text{and} \quad V''(R,Z) = \int_0^{\infty} c(k) k^2 U(R) e^{-kZ} dk \quad (12)$$

The arbitrary coefficient can now be evaluated because $V''(R,Z)$ is known along the boundary, $R = 1$. Therefore

$$V''(1,Z) = \int_0^{\infty} c(k) k^2 e^{-kZ} dk = \frac{4\alpha}{9} Z^{-2/3}. \quad (13)$$

This equation is well behaved and is conveniently in the form of a Laplace transformation, so that it is easily solved for $c(k)k^2$

$$c(k)k^2 = 4\alpha \left\{ 9\Gamma\left(\frac{2}{3}\right) k^{1/3} \right\} \quad (14)$$

where $\Gamma\left(\frac{2}{3}\right)$ is the gamma function of $2/3$. One may now rewrite the equation for both $V''(R,Z)$ and $V''(1,Z)$ and subtracting one from the other

$$V''(R,Z) = \frac{4\alpha}{9} Z^{-2/3} + \int_0^{\infty} \frac{4\alpha}{9\Gamma\left(\frac{2}{3}\right)} \frac{1}{k^{1/3}} \{U(R) - 1\} e^{-kZ} dk. \quad (15)$$

Integrating this expression twice, one obtains

$$V(R,Z) = \alpha Z^{4/3} + \int_0^{\infty} \frac{4\alpha}{9\Gamma\left(\frac{2}{3}\right)} \frac{1}{k^{7/3}} \{U(R) - 1\} e^{-kZ} dk + F_1(R)Z + F_2(R). \quad (16)$$

The last two terms are generated as integration constants. As $V(R,Z)$ must obey Laplace's equation for every $R > 1$, $Z > 0$; then $F_2(R) = K_2 \ln R$ and $F_1(R) = K_1 \ln R$. However, our boundary conditions also stipulate that $\frac{\partial V}{\partial R}(R,Z) = 0$ at $R = 1$ for all Z ; therefore K_2 and K_1 must both equal zero.

Our final equation for the potential distribution outside of the beam needed in order to support the $4/3$ power potential gradient is

$$\frac{V(R,Z)}{\alpha} = Z^{4/3} + \int_0^{\infty} \frac{4}{9\Gamma\left(\frac{2}{3}\right)} \frac{1}{k^{7/3}} \{U(R) - 1\} e^{-kZ} dk. \quad (17)$$

$R \geq 1, Z \geq 0$

Attempts to solve this expression analytically have not been productive, and although solutions in the form of numerous infinite series are possible, the convergence is often so slow as to make the process untenable. However, as the integrand is well-behaved for all values of k , the formulation is subject to easy analysis by computer. Figure 3 is the result of computer runs showing the plot of R versus Z for various equipotential values of $V(R,Z)/\alpha$. Also, the values as measured many years ago by Pierce are shown by the dark lines on this plot. The agreement is quite good considering the accuracy which might be expected from the experimental electrolytic tank measurements.

Zero Potential Cone Angle

The shape of the zero equipotential surface for large values of R becomes conical in shape. The cone angle has been calculated by Spangenberg,⁵ 71° ; and by Lapostolle,⁶ $74^\circ 10'$. In the latter case, the field distribution was calculated for a line of charge having the $4/3$ power potential gradient and should correspond to our case for $R > 1$. Setting $\frac{V(R,Z)}{\alpha}$ equal to zero in equation (17)

$$Z^{4/3} = - \frac{4}{9\Gamma\left(\frac{2}{3}\right)} \int_0^{\infty} \frac{1}{k^{7/3}} \{U(R) - 1\} e^{-kZ} dk. \quad (18)$$

For values of $R \gg 1$, $Z \gg 1$, $U(R)$ can be approximated by letting $k \rightarrow 0$ in $U(R)$, but not kR . Thus, $U(R) \approx J_0(kR)$ and one can rewrite equation (18)

$$Z^{4/3} = - \frac{4}{9\Gamma\left(\frac{2}{3}\right)} \int_0^{\infty} \frac{1}{k^{7/3}} \{J_0(kR) - 1\} e^{-kZ} dk. \quad (19)$$

Again, this expression has not yielded to an analytical solution and one is forced to make further approximations or to put it on the computer. Our approach has been to do both. The angle as measured off the computer field plots is 74° . If $J_0(kR) - 1$ is approximated by $\left(\frac{kR}{2}\right)^2$, the first term in the power series expansion, one can solve the resulting equation and finds $\frac{R}{Z} = 3$ or $71^\circ 33'$. However, if one tries to include more terms in the power series, the answer varies radically depending on the number of terms, indicating the integral of the series does not converge. One is led to other types of approximations. For example if one lets

$$J_0(kR) - 1 \cong - \left(\frac{kR}{2}\right)^2 e^{-\frac{kR\beta}{2}} - \beta \left(\frac{kR}{2}\right)^3 e^{-\frac{kR\gamma}{2}} \quad (20)$$

where $\beta = \left[\frac{\sqrt{3}}{2(2-\sqrt{3})} \right]^{1/2}$ and $\gamma = \left[\frac{1}{2\sqrt{3}(2-\sqrt{3})} \right]^{1/2}$ and then solves equation (19), the resulting

transcendental equation can be evaluated and $\frac{R}{r} = 3.42$ or a cone angle of $73^{\circ}45'$. Equation (20) is equivalent to a two-term approximation, converges, and is Laplace-transformable. As it turns out, equation (20) is not valid for large kR , but then $J(kR)$ does not contribute to the integration for large kR . At this stage of theoretical development various analytical solutions will be subject to different approximations, which can vary slightly the resulting cone angle. Equation (20) appears to be in agreement with the computer measured angle of $74^{\circ} \pm 1/4^{\circ}$.

Accelerating Column

As an example of the "Pierce" Geometry, Fig. 4 illustrates a cross section of the extraction region of the preliminary design of an accelerating column for the Los Alamos Meson Facility. The column is designed for 50 milliamperes and a beam radius of 0.7 cm. The equipotential electrodes are to be built of Ti-6Al-4V alloy and the maximum potential gradient, which is at the exit end of the column, is approximately 30 KV/cm. The ceramic rings and Ti alloy electrodes will be vacuum brazed in a manner similar to that employed by Klystron tube manufacturers, that is, the ceramic and Ti alloy will have matched temperature coefficients and will be sealed at high temperatures (950°C) by reactive metal brazing. The supporting structure for the equipotential electrodes are truncated cones of the same Ti alloy and are perforated by holes to aid in the hydrogen pumping problem. The holes will be staggered from support to support to prevent a continuous path for secondary electrons through the entire column. Visual access from the beam to the ceramic spacers is denied by the orientation of these support structures.

Finite Emittance

It is extremely difficult to include a finite emittance into the beam and to carry out a similar type of analysis to determine the optimum current density distribution and optimum accelerating potential distribution to minimize the growth of effective emittance. Assumption of finite emittance patterns implies knowledge of phase space distributions and its interplay with real space density distributions. This knowledge is lacking. However, it is quite evident that a finite emittance will eventually degrade an initially uniform current density distribution unless the emittance has a very specific, non-realistic, phase space distribution as determined, for example, by Kapchinskij and Vladimjirskij⁷ for the non-accelerated beam, and by Ohnuma⁸ for the accelerated beam. If we make the assumption that the normalized emittance is more or less constant during the acceleration through the column, we can follow the procedure of Walsh⁹ and add a term to the right-hand side of equation (1) to include the emittance, \mathcal{E} , where r is now changed to R , the outer radius of the beam, and the density distribution is assumed to be constant. The added term is

$$- e^2 \left[1 + R'(z)^2 \right] / 2V(z) e m_0 R^3(z). \quad (21)$$

Equation (1) with the above additional term gives the motion of the envelope of the beam through the accelerating column. It is easy to compare the added term of the equation, containing the emittance factor, with the other terms of equation (1) containing the current factor. The emittance term is usually very small (two orders of magnitude) as compared to the current term for most of the recent accelerating column designs. Thus the emittance term can be neglected in determining the accelerating potential distribution and equation (7) can be used with confidence knowing that one is not doing any great violence to the concept of maintaining a very low effective emittance.

Summary

The Child-Langmuir law has been solved in a rather roundabout manner, including the external fields necessary to maintain the $4/3$ power potential gradient; but in so doing the facts are established that in order to maintain a zero effective emittance during acceleration, the beam must be: a) formed in a magnetic field free region at the plasma boundary; b) extracted from the plasma surface with a uniform density distribution; and c) accelerated according to the $4/3$ power potential gradient.

It may be well to point out that even if r' and r'' are not zero (but still $r'' \ll 1$, giving a "Pierce"-like geometry) equation (1) will still allow the scale change criteria $r \rightarrow ar$ without changing equation (1) too much. However, slight changes in the density distribution have a much more pronounced effect and will lead to more serious emittance warping. It would appear that a uniform density distribution should be the primary objective in a low emittance column design with as near a "Pierce" geometry extraction system as practical. In addition, the beam should be extracted from the plasma surface in as near a magnetic field free region as possible.

Acknowledgments

I would like to acknowledge the contributions of various staff members of Los Alamos Scientific Laboratory for their contributions: Blair Swartz for his advice concerning the theoretical development, particularly in pointing out the convenient form of equation (11); Ken Crandall for translating the external field problem to the computer; and Tony Damiano for the mechanical design of the accelerating column.

References

1. D. H. Menzel, Fundamental Formulas of Physics, Prentice-Hall, Inc. 1955, p. 438.
2. J. W. Beal, Beam Trajectories Under the Influence of Self-Fields and External Focusing Elements, Lawrence Radiation Laboratory Report UCRL 14194 (May 1965).
3. J. R. Pierce, Theory and Design of Electron Beams, D. Van Nostrand Co. Inc. (1949), pp. 168-175.
4. P. Lapostolle, A. Blanc-Lapierre, and G. Goudet, Electronique General, Editions Eyrolles (1959) pp. 326-330.
5. K. R. Spangenberg, Vacuum Tubes, McGraw-Hill Book Co., Inc. (1948), p. 452.
6. P. Lapostolle, Private communication and also reference 4 above.
7. I. M. Kapchinskij and V. V. Vladimirsij, Conference of High-Energy Accelerators and Instrumentation, CERN, Geneva (1959), p. 274.
8. S. Ohnuma, On a Uniform Charge Density of a Beam and its Phase-Space Distribution, Yale University Internal Report, Y-16 (Sept. 16, 1966).
9. T. R. Walsh, Plasma Physics (Journal of Nuclear Energy, Part C), Vol. 5, pp. 17-22.

DISCUSSION

C. R. EMIGH, LASL

LEFEBVRE, Saclay: I just want to say that, experimentally, we have found the density distribution to be an extremely sensitive factor for the beam quality. We found that slight modifications of the expansion cup geometry greatly influence the density distribution at the extraction level.

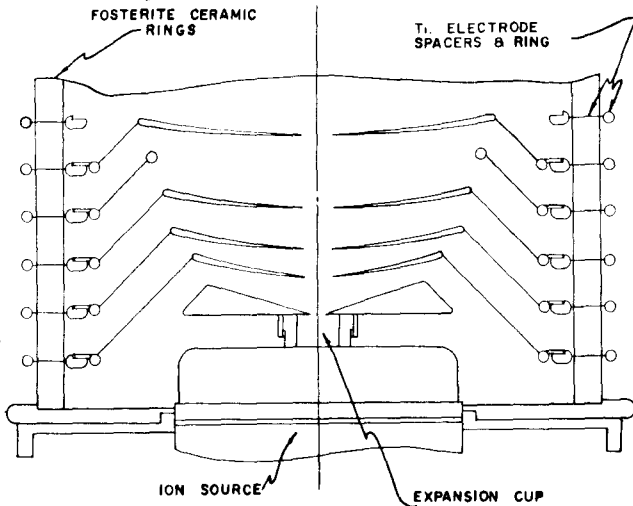


Fig. 4. Partial accelerating column design.

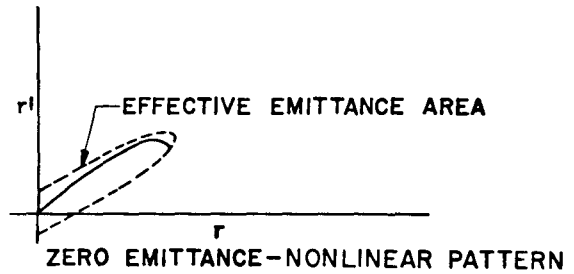
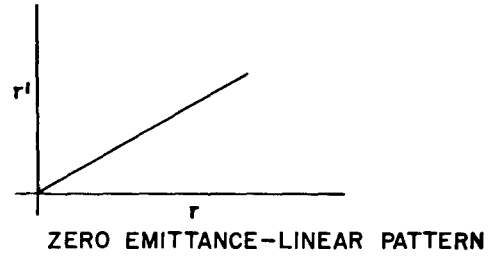


Figure 1.

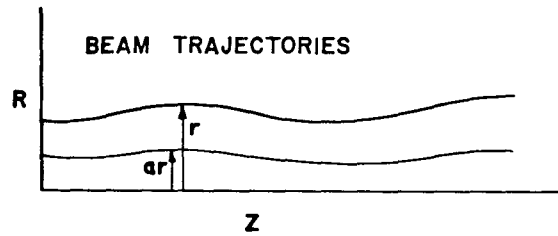


Figure 2.

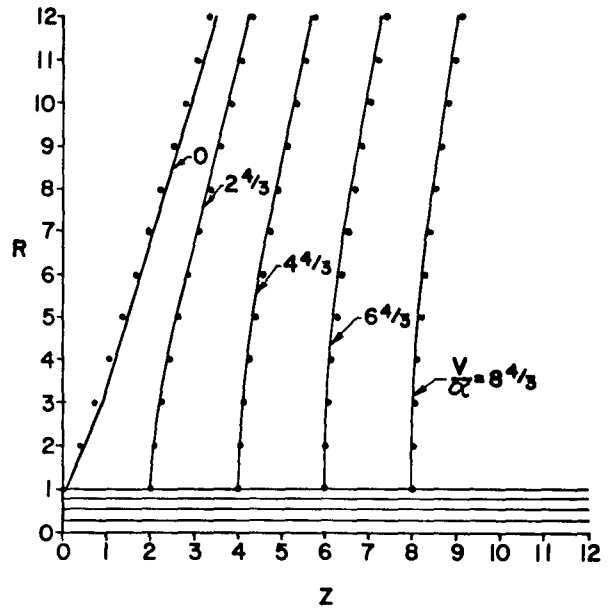


Fig. 3. Pierce geometry external field pattern.